

A Semi-Supervised Approach for Abnormal Event Prediction on Large Operational Network Time-Series Data

Yijun Lin and Yao-Yi Chiang

lin00786@umn.edu, yaoyi@umn.edu

Department of Computer Science and Engineering
University of Minnesota, Twin Cities

Abstract

Large network logs, recording multivariate time series generated from heterogeneous devices and sensors in a network, can often reveal important information about abnormal activities, such as network intrusions and device malfunctions. Existing machine learning methods for anomaly detection on multivariate time series typically assume that 1) normal sequences would have consistent behavior for training unsupervised models, or 2) require a large set of labeled normal and abnormal sequences for supervised models. However, in practice, normal network activities can demonstrate significantly varying sequence patterns (e.g., before and after rerouting partial network traffic). Also, the recorded abnormal events can be sparse. This paper presents a novel semi-supervised method that efficiently captures dependencies between network time series and across time points to generate meaningful representations of network activities for predicting abnormal events. The method can use the limited labeled data to explicitly learn separable embedding space for normal and abnormal samples and effectively leverage unlabeled data to handle training data scarcity. The experiments demonstrate that our approach significantly outperformed state-of-the-art approaches for event detection on a large real-world network log.

Keywords: semi-supervised learning, multivariate time series, network event prediction

1 Introduction

Nowadays, many network management companies (e.g., Cisco, NTT Global Networks) collect large volumes of data logs to measure and monitor the status (e.g., healthy, overloaded, power outage) of devices (e.g., routers, switches) or interfaces (e.g., local area networks (LAN), wide area networks (WAN)) in a network. Figure 1 shows an example network. A network usually consists of multiple devices, each with some interfaces, e.g., an SDWAN device has LAN and WAN interfaces.

Each interface is measured by several metrics or attributes, i.e., the number of in/out octets and in/out ucast packets, that describe network operations or activities as multivariate time series.

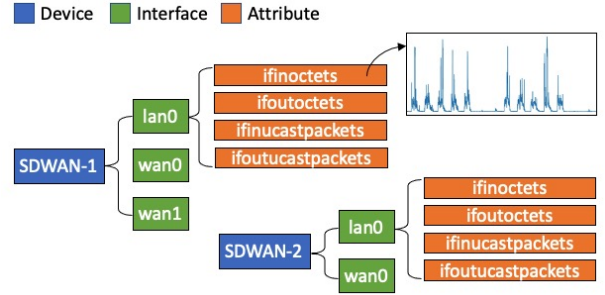


Figure 1: An example network contains two SDWAN devices, and the devices have some LAN and WAN interfaces, each measured by four attributes.

Efficiently and accurately predicting abnormal events from network data logs is important, which helps continuously monitor network states and raise alerts for potential incidents on time for network engineers to investigate and resolve. Traditional monitoring systems typically trigger a real-time notification when the network is experiencing some abnormal event (e.g., packet loss, intrusion) using pre-defined rules but cannot provide an early warning on a potential incident. Also, a network typically contains hundreds if not thousands of heterogeneous devices from different vendors, which can have diverse criteria (e.g., some rules and thresholds) indicating varying levels of abnormal status, making it challenging to build an early warning system and enable the system handling all kinds of networks.

Advanced data-driven methods on analyzing *multiple multivariate time series* (e.g., machine learning approaches) can automatically learn and extract patterns from network operations that lead to a potential abnormal event, which has the potential to handle het-

erogeneous networks, devices, and interfaces. One challenge is how to effectively capture temporal dependencies across time and relationships between time series that can jointly represent network activities for predicting an abnormal event. Some existing approaches overlook the relationships between time series, e.g., univariate time-series anomaly detection algorithms [16], fusing multiple time series directly as features [12, 10]. In terms of modeling temporal dependencies, many approaches use recurrent neural networks (RNNs) [12, 8] yet they are often time-consuming and require large memory for computation. Transformers, oriented from natural language processing, become popular in time-series analysis problems [1], but they have similar issues.

In addition, some labeled data might be available, but the labeling criteria could vary significantly among devices and interfaces, e.g., an abnormal event can last for several minutes, and sometimes only the beginning time point is marked as anomalous. Unsupervised approaches, including reconstruction-based methods [14, 21], forecasting-based methods [9, 8], and hybrid methods [29], identify infrequent behaviors in multivariate time series as an anomaly. However, this assumption is not always true, e.g., long-term peak usage of memory might be rare but normal. Supervised models [11, 19] can leverage labeled data to guide the process of learning the time-series patterns leading to an abnormal event, but they usually require sufficient labeled samples. Also, the number of labeled abnormal samples is usually much smaller compared to the normal samples. Therefore, limited and imbalanced labels make it challenging to capture the patterns leading to abnormal activities.

This paper proposes a semi-supervised learning approach that learns representative features for network activities and use the features to predict abnormal events (e.g., packet loss, intrusion). Specifically, our approach first takes a given network and constructs a graph representation where each node contains some attributes of an interface (e.g., packet volume) at a time point. (There could be some dependencies (e.g., data transmission) between interfaces (nodes) via the linkage.) Considering a sequence of graphs (i.e., network data logs over a time period) leading to some abnormal event, our approach aims to generate an embedding to represent network behaviors and capture the unique pattern of this graph sequence. The embedding should contain effective temporal information by capturing temporal dependencies across time points (i.e., temporal patterns). The embedding also includes relevant information from neighboring nodes, capturing data communication patterns. Therefore, our approach jointly captures temporal dependencies across

time points and spatial dependencies between nodes for generating an embedding of the input. Then these learned embeddings are refined to form two separable clusters representing normal and abnormal network behaviors. Our approach uses labeled samples to explicitly learn the cluster centers in a contrastive way. However, due to imbalanced and limited labeled samples, the learnt centers might not be applicable to all samples and hence poor embedding quality. Our approach updates the embeddings of all samples towards a high confidence clustering distribution to enforce cluster cleanliness with a semi-supervised learning strategy. The goal is to improve separability between normal and abnormal network behaviors. Finally, our approach utilizes a support vector classifier on these embeddings to predict if the given graph sequence of network operations will lead to an abnormal event.

In sum, the main contribution of this paper is a semi-supervised learning approach that learns separable embeddings that jointly captures temporal dependencies between time points and relationships between time series for predicting abnormal events. The proposed approach can efficiently capture complex dependencies in multiple multivariate time-series data and learn effective features from imbalanced and limited labels, enabling accurate prediction of abnormal events. We demonstrate the proposed network architecture for abnormal event prediction on large real-world network operation time-series data.

2 Methodology

2.1 Problem Definition Given a network containing multiple interfaces with unknown connectivity, our system first constructs a fully-connected graph, $\mathbf{G} = (\mathbf{V}, \mathbf{E})$, where each node $i \in \mathbf{V}$ represents an interface ($|\mathbf{V}| = n$) and the connection between any pair of nodes is initialized as one, meaning there can be data communication between interfaces. Let $\mathbf{G}^{(t)} \in \mathbb{R}^{n \times F}$ be the graph for network operation measurements at time t , where n is the number of nodes and F is the number of attributes describing each node. Suppose the input is a sequence of graphs of length T , i.e., graphs from $t - T + 1$ to t , our approach aims to learn a function f that maps T historical input signals to a binary signal $y \in \{0, 1\}$ indicating if there will be an abnormal event in the network at $t + 1$.

$$[\mathbf{G}^{(t-T+1)}, \dots, \mathbf{G}^{(t)}] \xrightarrow{f} y$$

Figure 2 shows the proposed network architecture for learning feature embeddings from the graph input. Specifically, our approach first builds an GatedConvNGAT module to generate an initial feature embedding

by jointly capturing dependencies among graphs (across time points in the sequence) and between nodes (between individual time series in a graph) (Section 2.2). Then our approach jointly refines the embeddings and cluster centers representing normal and abnormal activities by: (1) leveraging *labeled* normal and abnormal samples to form clusters in a contrastive learning way; (2) improving the separability of clusters using both *labeled* and *unlabeled* samples in a semi-supervised manner (Section 2.3). Finally, our approach trains a support vector classifier with these learned embeddings for the prediction task (Section 2.4).

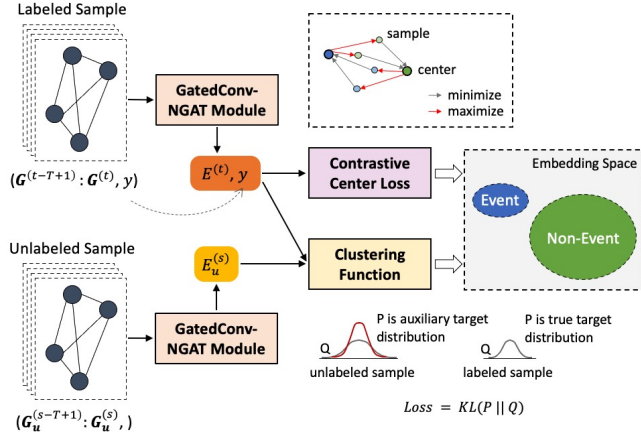


Figure 2: The training process of our system to generate feature representation for predicting abnormal events

2.2 GatedConv-NGAT Module. This section introduces the ST-Conv-NGAT module that generates embeddings from the input graph sequence (Figure 3). In general, the module contains temporal gated convolutional layers to capture temporal dependencies across time and a normalized graph attention layer to capture dependencies between nodes. The details of each submodule are described as follows.

GatedConv layer for extracting temporal relationships. Recurrent neural networks (RNNs), e.g., long short-term memory (LSTM), have been widely used for capturing temporal dependencies in time-series data, but these models typically suffer from complex gating mechanisms, time-consuming computation, and large memory requirement since every step relies on the previous steps. In comparison, convolutional neural networks (CNNs) have the advantages of fast training and parallel computation [7] that can process large network data logs more efficiently. Also, CNNs explicitly capture local features within a temporal neighborhood, and one or more local features might cause an abnormal event, instead of global features from the entire sequence.

Our approach applies gated-conv layers [7] with

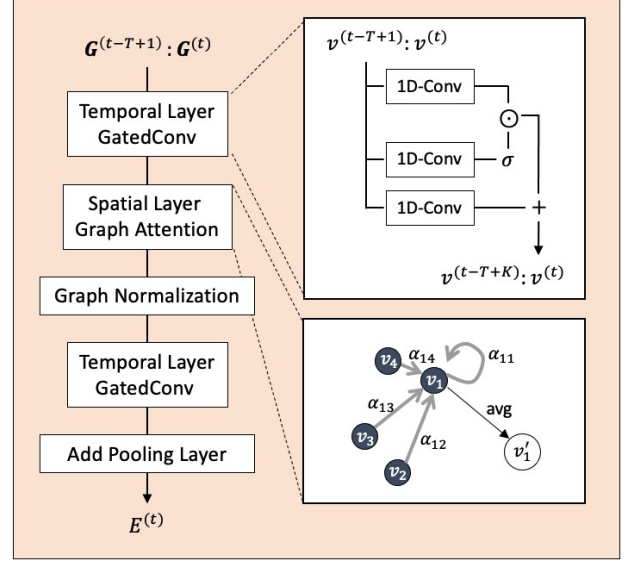


Figure 3: GatedConv-NGAT Module

multiple kernel sizes consisting of 1D convolution operations on the time axis to extract local temporal features for each node. The input to the 1D convolution operation is a sequence of length T with a channel size F at each node $\in \mathbb{R}^{T \times F}$. With a kernel size K and a hidden size C , the convolution kernel maps the input to the output $[\mathbf{m} \ \mathbf{n}] \in \mathbb{R}^{(T-K+1) \times (2C)}$, where \mathbf{m} , \mathbf{n} split the output into halves with the same hidden size h . The gated-conv layer leverages gated linear units (GLU) [3] as a non-linear gating mechanism over \mathbf{m} and \mathbf{n} :

$$(2.1) \quad \text{GatedConv}(\mathbf{v}) = \mathbf{m} \odot \sigma(\mathbf{n}) \in \mathbb{R}^{(T-K+1) \times (C)}$$

where \mathbf{m} and \mathbf{n} are the input to the gates of GLU, \odot denotes the element-wise product, σ is the sigmoid function, and $\sigma(\mathbf{n})$ controls which information in \mathbf{m} are relevant for generating temporal features.

Normalized graph attention layer for extracting relationships between nodes. After the first Gated-Conv layer, each node i is represented by $(T - K + 1)$ feature vectors of size C , where each vector contains the extracted temporal features for the corresponding sub-sequence. In addition to temporal dependencies, combining information from other nodes is also essential for determining an abnormal event. Thus, our approach introduces a normalized graph attention layer to capture relationships between nodes.

Since the initial graph topology is unknown, many graph convolution strategies, e.g., chebyshev spectral graph convolutional operator [4], might not be suitable because they require the graph connectivity as the input. Our approach leverages a graph attention (GAT) layer [23] to model the spatial relationships between nodes. A GAT layer computes the representation for

each node:

$$(2.2) \quad \text{GAT}(i) = \sigma \left(\sum_{k \in \mathcal{N}_i} \alpha_{ik} \mathbf{v}_k \right)$$

where node i is the target node, $\mathbf{v}_i \in \mathbb{R}^C$ is the hidden feature vector of node i , \mathcal{N}_i is the neighborhood set of node i , σ is the sigmoid function, α_{ik} is the attention score for node k to node i . The attention score α_{ik} is defined by:

$$(2.3) \quad \alpha_{ik} = \frac{\exp(\sigma(\mathbf{w}^T \cdot (\mathbf{v}_i \parallel \mathbf{v}_k)))}{\sum_{j \in \mathcal{N}_i} \exp(\sigma(\mathbf{w}^T \cdot (\mathbf{v}_i \parallel \mathbf{v}_j)))}$$

where the operation \parallel is to concatenate two vectors, $\mathbf{w} \in \mathbb{R}^{2C}$ is a learnable weight vector, \mathcal{N}_i is the neighborhood set of node i , σ is the LeakyReLU function.

Our approach then adapts graph normalization (GraphNorm) [2] to the output of the GAT layer, which makes the optimization more efficient. GraphNorm normalizes every feature dimension for individual graphs with a learnable shift, which significantly boosts the training upon InstanceNorm [22] (also does graph-targeted normalization):

$$(2.4) \quad \text{GraphNorm}(h_{i,j}) = \gamma_j \cdot \frac{h_{i,j} - \alpha_j \mu_j}{\sigma_j} + \beta_j$$

$$\mu_j = \frac{\sum_{k=1}^n h_{k,j}}{n}, \quad \sigma_j = \frac{\sum_{k=1}^n (h_{k,j} - \alpha_j \mu_j)}{n}$$

where $h_{i,j}$ is the value of the j th feature dimension of $\text{GAT}(i)$ (the output of GAT layer for node i), n is the number of nodes in the graph, α_j is the learnable parameter for the feature dimension j , which controls how much information to keep in the mean. γ_j and β_j are the affine parameters.

Putting everything together to learn embeddings. Inspired by [28], our approach adds another temporal gated-conv layer after the NGAT layer to fuse the features of node interactions on the time axis. This “sandwich” structure (i.e., a spatial layer in the middle of two temporal layers) can achieve fast spatial-state propagation through temporal convolutions. After the second temporal gated-conv layer, our approach concatenates the output to generate the node embeddings. Then our approach uses a global pooling layer to add node embeddings across the node dimension to generate the graph embedding. In this way, given $[\mathbf{G}^{(t-T+1)}, \dots, \mathbf{G}^{(t)}] \in \mathbb{R}^{T \times n \times F}$, the GatedConvNGAT module generates the embedding $\mathbf{E}^{(t)}$ of length $(T - 2(K - 1)) \times C$, that jointly captures the temporal dependencies and relationship between nodes.

2.3 Learning clustering structure. Our approach assumes two clusters in the embedding space: normal

and abnormal events. The goal is to learn a representation space to form these two separable clusters.

Learning clustering structure on labeled samples using contrastive center loss. The labeled samples can explicitly guide the process of learning clustering centers by enforcing the embeddings of normal samples to be close to the normal center and far away from the abnormal center, and vice versa. Our approach applies the contrastive-center loss [15] that considers intra-class compactness and inter-class separability simultaneously. This loss function aims to penalize the contrastive values between (1) the distances of samples to their corresponding class center and (2) the distances of samples to their non-corresponding class centers,

$$(2.5) \quad \mathcal{L}_{cc} = \frac{1}{2} \sum_{i=1}^m \frac{\|\mathbf{E}_i - \mathbf{c}_{y_i}\|_2^2}{\|\mathbf{E}_i - \mathbf{c}_j\|_2^2 + \epsilon} \quad (j \neq y_i)$$

where \mathcal{L}_{cc} denotes the contrastive-center loss; m is the number of labeled samples in a min-batch; \mathbf{E}_i is the embedding of the i -th training sample; \mathbf{c}_{y_i} is the corresponding center of \mathbf{E}_i . Since there are two clusters, when y_i is 0, j is 1, and vice versa ($j \neq y_i$). ϵ is a constant for preventing the denominator equal to 0 and set to $1e-6$ empirically.

Learning clustering structure on all samples using a semi-supervised learning strategy. Using the contrastive learning strategy improves the clustering cleanness for labeled samples; however, due to limited and imbalanced labeled samples, the learned centers are easily guided by the given labeled samples, which might fail in inferencing. To overcome the scarcity of labeled training samples and ensure the clusters are applicable to all samples, our approach takes the idea from [27] to minimize the distance between the cluster assignment and some target cluster distribution. For labeled samples, the target distribution can be directly derived from the label, while for the unlabeled samples, the target distribution is derived from high confidence predictions of the current cluster distribution from all samples. Formally, our approach calculates the probability of assigning the embedding \mathbf{E}_i to the cluster j with a center μ_j as

$$(2.6) \quad q_{ij} = \frac{(1 + \|\mathbf{E}_i - \mu_j\|^2)^{-1}}{\sum_{j'} (1 + \|\mathbf{E}_i - \mu_{j'}\|^2)^{-1}}$$

Following the work in [27], our approach derives an auxiliary distribution made up of the high confidence assignments of the current distribution (referred as Q). The main idea is to emphasize data points assigned with high confidence to ensure cluster purity. Equation 2.7 defines the computation of auxiliary distribution (referred as P), where the second power of q_{ij} places more weight on the instances near the center and the division

of $\sum_i q_{ij}$ normalizes based on the cluster size, making the model robust to biased classes. Note that for labeled samples, our approach replaces the true distribution with the auxiliary distribution and hence enables the training process in a semi-supervised manner.

$$(2.7) \quad p_{ij} = \frac{q_{ij}^2 / \sum_{i'} q_{i'j}}{\sum_{j'} (q_{ij'}^2 / \sum_{i'} q_{i'j'})}$$

To measure the distance between the distributions P and Q , our approach computes the KL divergence to measure their distance. The clustering oriented loss is defined as,

$$(2.8) \quad \mathcal{L}_{KL} = KL(P||Q) = \sum_i \sum_j p_{ij} \log \frac{p_{ij}}{q_{ij}}$$

Therefore, the total loss is the sum of contrastive center loss and KL divergence loss with a hyper-parameter λ ,

$$(2.9) \quad \mathcal{L} = \mathcal{L}_{cc} + \lambda \times \mathcal{L}_{KL}$$

2.4 Predicting abnormal events from learned embeddings using SVC. Using the methods described so far in this section, our model generates separable embeddings (normal vs. abnormal). Then we take the embeddings and labels to train a support vector classifier to predict normal and abnormal events. Our approach does not train in an end-to-end manner, e.g., using a fully-connected layer for classification in the model because support vector classifier usually works better if the input are already separable in some space. Figure 4 shows the prediction process. Given a sequence of graphs representing network operations, the GatedConv-NGAT module generates the embedding and the support vector classifier takes the embedding to predict if the input would lead to an abnormal event.

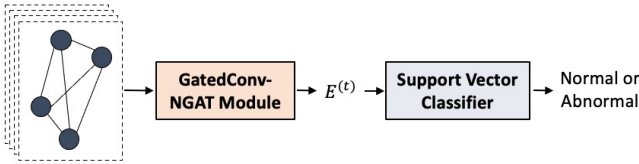


Figure 4: Event prediction

3 Experiments and Results

We implemented the proposed architecture with Python 3.8, PyTorch 1.8, and PyTorch Geometric framework [6]. We conducted the experiments in a Docker container deployed on a GPU server and trained the model with one physical core and 16GB memory.

3.1 Datasets. We used the network operation data from NTT-GN for the experiments. The dataset con-

tains more than 150 million data logs from network interfaces (e.g., WAN routers and LAN switches) that NTT-GN collects, monitors, and manages. The data logs we used cover the time range from 2020-05-12 to 2020-06-12, with a time interval of 5 minutes. Figure 1 shows an example of the data structure. In this work, we assume a practical case that there could be dependencies between any interface pairs in a network (e.g., data transmissions) (Figure 5(a)), and the network topology is not available. The graph representation can be modified if prior knowledge of the network topology is available.

In addition to the network operation data, NTT-GN also provides the packet loss event dataset that reports the ticket opening time at the device level. We assume that events are caused by some abnormal network activities in the network and can be captured by looking at the dynamics of the entire network. Figure 5(b) shows an example of assigning a label to a period of network activities (e.g., 6 hours, a sequence of 72 graphs). If there is an event reported at t' and the closest graph before that is $\mathbf{G}^{(t)}$, we assigned label 1 (color blue) to the graph sequence $\mathbf{G}^{(t-71)} : \mathbf{G}^{(t)}$, denoting that these graphs contains some abnormal network activities directly leading to an event. Since we do not know how long the event lasts, the graph sequences overlapped with an event within 6 hours before and after (e.g., color yellow) were marked as “unknown” (i.e., unlabeled data). These graph sequences also help learn feature embeddings in our semi-supervised setting. The rest graph sequences that do not overlap with any event within 6 hours were labeled as 0, representing normal network activities.

3.2 Experiment Settings. To evaluate the proposed approach, we selected the available networks with at least 50 events. We split the samples into training, validation, and testing sets, ensuring each set contains both label 0 and label 1. Table 1 shows the summary of the dataset. We observe that the number of samples labeled with 0 is much larger than label 1. Also, the ratio of labeled samples to unlabeled samples is around 0.2. We repeated the random splitting process three times for cross-validation and took the average as the results.

We set the length of the input graph sequence in a sample as 72. The batch size was 32, each containing both labeled and unlabeled samples. We set the temporal gated convolutional layers as 32 hidden states and the kernel size of 1D Conv as 12. The size of the output feature embeddings was 256. The initial learning rate was 0.001, with early stopping on the validation dataset. The hyper-parameters were chosen by grid search on the validation set, and we reported

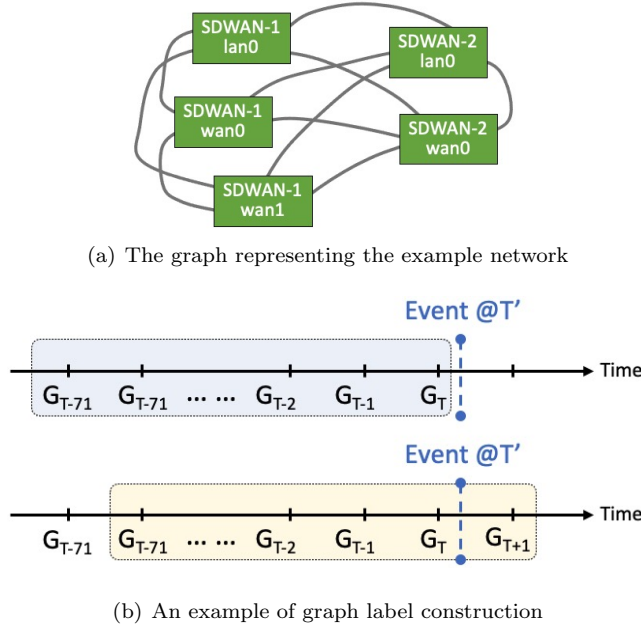


Figure 5: Examples of sample construction

the results with the set of hyper-parameters yielding the best average performance, that is $\lambda = 0.1$.

Table 1: Summary of the datasets

Network ID	#Nodes	#Events	# 0: # 1
1NTT18927	53	125	0.96:0.04
1NTT19535	84	142	0.89:0.11
1NTT67246	36	134	0.91:0.09
1NTT19478	120	147	0.88:0.12
143XB8CT	97	78	0.98:0.02
1NTT30990	20	71	0.98:0.02
1NTT48337	89	83	0.95:0.05
1NTT19213	119	78	0.96:0.04
1NTT22885	91	91	0.95:0.05
1NTT18635	143	189	0.73:0.27

Metrics. We reported the precision, recall, and F1 score for label 1 since our goal is to predict events. The higher the values the better the performance. We put the detailed functions in the supplementary file.

Baselines. We compared our proposed model to the following state-of-the-art baselines:

- Support Vector Classifier (SVC): We convert the problem to a binary classification task for SVC. We flatten an input graph sequence in time and node dimensions to be a large vector for predicting event or non-event.
- Graph Attention Encoder (GAT): We concatenate features along the temporal dimension for each

node and replace the encoder with only the graph attention module to capture interactions between time series. This method aims to demonstrate the necessity of capturing temporal dependencies.

- Graph Attention LSTM (GAT-LSTM) [25]: Instead of using the ST-Conv module, we apply LSTM in the encoder to capture interactions across time points. The rest architecture remains the same as our proposed approach.
- MTAD-GAT [29]: This is an unsupervised anomaly detection approach that explicitly captures relationships between multiple features and across time points. We modify the approach so that the node value has more than one dimension.
- DeepSAD [18]: This is a semi-supervised learning approach for anomaly detection that aims to learn a clustering center to represent normal cases. The original domain is computer vision. To extend the model on our dataset, we apply the ST-Conv-NGAT module as the encoder.
- We select the following variations of the proposed model for ablation study: 1. ST-Conv-NGAT + only contrastive center loss (only-CC), which would be trained only with labeled samples; 2. ST-Conv-NGAT + only KL divergence loss (only-KL); 3. Constructing a correlation graph as the input [5], which computes pairwise Pearson correlation between nodes and assumes two nodes are connected only if the correlation value is above the mean plus one std.

3.3 Model Performance. In general, our approach outperformed baseline methods in all networks (see F1 scores in Figure 6 and precision & recall in the supplementary file). The F1 scores in most networks are above 0.7. Even when the ratio between the number of label 0 and label 1 is high (e.g., “143XB8CT” and “1NTT30990”), our model could still achieve far better results than the baseline models. Specifically, our approach achieved more than 50% improvement in F1 scores compared to SVC. This is because SVC simply takes the input graph sequence as a flattened vector and does not explicitly capture relationships between time series or across time points.

Compared to using other encoding methods (GAT and GAT-LSTM) to generate representations for prediction, our approach with the ST-Conv-NGAT module as the encoder showed excellent advantage. First, GAT does not explicitly consider temporal dependencies but fuses features on the time dimension together and expects the model to extract useful information from these values for prediction directly. However, the temporal

order of these values matters for event prediction, e.g., the position of a sudden increment might result in different network behaviors. Our approach leverages the 1D-CNN to summarize local temporal features, aiming to extract effective temporal patterns leading to an event. Second, although GAT-LSTM is commonly used for capturing spatiotemporal dependencies in multi-time-series data [25], its performance is poorer than our approach, which might be because GAT-LSTM is typically generating representations for the entire time series. However, in practice, only some subsequence(s) from the input graph sequence would cause an event. Some effective patterns (or features) at the early stage of the input sequence might be easily weakened or neglected during the sequential training of LSTM. Since the impacting subsequence(s) on the event are unknown (i.e., the leading time to an event could be varying), the sequence length (i.e., six hours in the experiment) was chosen to cover as many time points as possible. In comparison, the 1D-CNN in our approach focuses on manipulating temporal interactions on every subsequence, which empirically fulfills our assumption and achieves better performance on real datasets. Also, training GAT-LSTM for one epoch took more than 600 seconds while our approach required around 170 seconds under the same settings.

Furthermore, compared to existing work on anomaly detection, our approach achieved better performance than the unsupervised learning approach (MTAD-GAT), which demonstrates that assuming rare samples as anomalies might not be applicable in practice. Adding some labeled samples during training can guide the learning process to generate representative embeddings. Additionally, our approach outperformed the semi-supervised approach, DeepSAD. DeepSAD has been demonstrated to outperform some unsupervised approaches in the original paper. The loss function in DeepSAD enforces labeled normal samples to be close to the predefined center and abnormal samples to be as far as possible. For the unlabeled samples, DeepSAD has a strong assumption that the majority of data samples are normal and treats all unlabeled samples as normal in the loss. However, such an assumption might not hold in practice since one event can last for some period (i.e., the unlabeled data might contain abnormal network activities), which might confuse the model to learn effective representations for unlabeled samples and result in poor performance.

3.4 Ablation Study. (1) Effect of Loss Functions. Table 2 shows that our approach achieved 12% improvement in F1 scores on average compared to only using the contrastive center (CC) loss and 14% improvement compared to only using the KL loss. The

model with only the CC loss was trained with limited labeled samples, which worked well for the networks with large abnormal samples (e.g., more than 120 events in “1NTT67246” and “1NTT18635”). However, the performance dropped in the cases with only a few abnormal samples. Our proposed approach trained on both labeled and unlabeled samples to force the learnt clustering structure was applicable to all data samples, resulting in better performance, e.g., 48% improvement in F1 score for “1NTT30990” and 35% for “1NTT19213”. In the other case, the model with only KL loss was trained with all samples. Without the CC loss to explicitly optimize the centers, finding good centers was challenging even when the true clustering distribution could be estimated from labeled samples.

(2) Effect of graph construction. We compared the result of the model taking input graphs constructed based on the correlations between nodes. However, the performance is generally worse than taking the fully-connected graph as the input, which shows that the node correlations could not effectively describe the interactions between interfaces. Since the network connectivity is unknown, the proposed approach assumes that data communication (direct and indirect) could happen between any interface pairs and uses the graph attention module to automatically capture their relationships. The entire results are presented as Table 2 in the supplementary file.

Table 2: F1 scores between using different loss functions (see the full table in the supplementary file)

Network ID	only-CC	only-KL	Ours
1NTT18927	0.809	0.717	0.823
1NTT19535	0.808	0.773	0.877
1NTT67246	0.955	0.889	0.946
1NTT19478	0.786	0.782	0.808
143XB8CT	0.462	0.466	0.502
1NTT30990	0.267	0.288	0.397
1NTT48337	0.757	0.672	0.754
1NTT19213	0.422	0.413	0.573
1NTT22885	0.800	0.850	0.897
1NTT18635	0.935	0.962	0.980

4 Related Work

There exists abundant literature on anomaly detection with time-series data. Deep learning approaches have shown promising results in capturing complex relationships between time series and across time points for extracting effective patterns that enable accurate anomaly prediction, including unsupervised [13, 5], supervised [11, 19], and semi-supervised approaches [24].

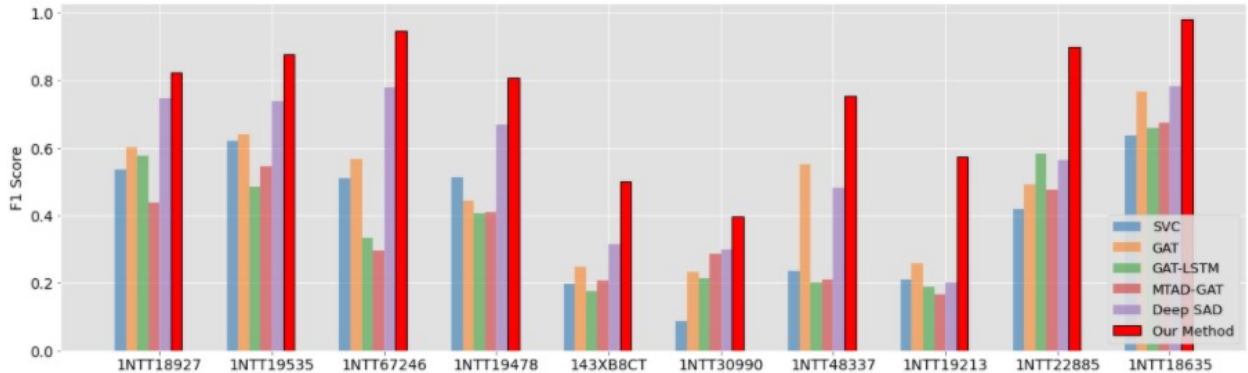


Figure 6: The F1 scores for baselines and our method (red). See precision and recall in the supplementary file.

For example, Hundman, Constantinou, Laporte, et al. [8] propose to use Long-Short-Term Memory (LSTM) to predict spacecraft telemetry and detect outliers in an unsupervised manner within each variable of a single multivariate time-series. However, the approach does not consider the dependencies between variables. Network operation data are typically multiple multivariate time-series data, which require careful considerations to capture the interactions between variables and time series for event detection. RNNs and Transformers [1] have been widely used in modeling temporal dependencies in time-series data, but they typically suffer from time-consuming training process and large memory requirement [28]. Zhao, Wang, Duan, et al. [29] propose an unsupervised anomaly detection approach on multivariate time-series data, with each variate/time series represented as one node in a graph. Their approach utilizes a feature attention layer and a temporal attention layer to explicitly capture the relationships between features and times respectively. Then the approach jointly optimizes a forecasting-based model and a reconstruction-based model to obtain better time-series representations. However, such unsupervised learning approaches usually make a strong assumption that infrequent behavior is anomalous and usually requires some scores for inference (e.g., see [17]). Although there are some techniques, e.g., Peak Over Threshold (POT) [20], that automatically determine the threshold during inference, the performance is still not competitive to supervised learning methods when labels are available (e.g., see [11, 19]). Supervised approaches can explicitly learn normal or abnormal patterns from labels yet requires a prohibitive large number of labeled examples (e.g., see [blazquez2021review]).

Semi-supervised learning approaches can overcome these limitations. For example, Ruff, Vandermeulen, Görnitz, et al. [18] demonstrates that adding a few labeled samples in a semi-supervised manner would guide the model to achieve better performance than unsuper-

vised learning methods for anomaly detection. Xiao, Guan, Zhao, et al. [26] propose a semi-supervised approach that uses an LSTM auto-encoder on both unlabeled data and labeled data with a reconstruction loss and adds prediction loss on the labeled data to guide the learning process. In comparison, our approach explicitly learns a separable embedding space for normal and abnormal samples instead of using a simple prediction loss (e.g., cross-entropy loss or focal loss for the imbalanced label situation). Vercruyssen, Meert, Verbruggen, et al. [24] propose a semi-supervised learning approach that first uses an unsupervised model, a clustering-based approach, to define typical normal behavior and identify anomalies. Then the approach actively adds labels from domain experts to guide the clustering approach in a semi-supervised manner. However, the performance would highly rely on the initialized clustering result. Our approach leverages the unlabeled samples to learn cluster centers in a self-learning way.

5 Conclusion

The paper presented a semi-supervised learning approach for predicting abnormal events from multiple multivariate time-series data. The proposed approach learns separable embeddings by leveraging labeled samples to learn cluster centers in a contrastive way and enforces unlabeled samples to follow similar clustering distribution to the labeled samples in a semi-supervised manner. We plan to explore methods for further detecting the event root cause, for example, determining the devices or interfaces and their activities leading to an event. Another direction is to take advantage of other networks in a transfer learning way when the labeled data is scarce.

6 Acknowledgement

This material is based upon work supported in part by the NTT Global Networks and NVIDIA Corporation.

References

- [1] L. Cai, K. Janowicz, G. Mai, et al. “Traffic transformer: Capturing the continuity and periodicity of time series for traffic forecasting”. In: *Transactions in GIS* 24.3 (2020), pp. 736–755.
- [2] T. Cai, S. Luo, K. Xu, et al. “Graphnorm: A principled approach to accelerating graph neural network training”. In: *ICML*. 2021, pp. 1204–1215.
- [3] Y. N. Dauphin, A. Fan, M. Auli, et al. “Language modeling with gated convolutional networks”. In: *ICML*. 2017, pp. 933–941.
- [4] M. Defferrard, X. Bresson, and P. Vandergheynst. “Convolutional neural networks on graphs with fast localized spectral filtering”. In: *NeurIPS* 29 (2016), pp. 3844–3852.
- [5] A. Deng and B. Hooi. “Graph neural network-based anomaly detection in multivariate time series”. In: *AAAI*. Vol. 35. 5. 2021, pp. 4027–4035.
- [6] M. Fey and J. E. Lenssen. “Fast Graph Representation Learning with PyTorch Geometric”. In: *ICLR Workshop on Representation Learning on Graphs and Manifolds*. 2019.
- [7] J. Gehring, M. Auli, D. Grangier, et al. “Convolutional sequence to sequence learning”. In: *ICML*. 2017, pp. 1243–1252.
- [8] K. Hundman, V. Constantinou, C. Laporte, et al. “Detecting spacecraft anomalies using lstms and nonparametric dynamic thresholding”. In: *ACM SIGKDD*. 2018, pp. 387–395.
- [9] N. Laptev, S. Amizadeh, and I. Flint. “Generic and scalable framework for automated time-series anomaly detection”. In: *ACM SIGKDD*. 2015, pp. 1939–1947.
- [10] D. Li, D. Chen, B. Jin, et al. “MAD-GAN: Multivariate anomaly detection for time series data with generative adversarial networks”. In: *ICANN*. 2019, pp. 703–716.
- [11] D. Liu, Y. Zhao, H. Xu, et al. “Opprentice: Towards practical and automatic anomaly detection through machine learning”. In: *IMC*. 2015, pp. 211–224.
- [12] P. Malhotra, A. Ramakrishnan, G. Anand, et al. “LSTM-based encoder-decoder for multi-sensor anomaly detection”. In: *arXiv preprint arXiv:1607.00148* (2016).
- [13] M. Munir, S. A. Siddiqui, A. Dengel, et al. “Deep-AnT: A deep learning approach for unsupervised anomaly detection in time series”. In: *IEEE Access* 7 (2018), pp. 1991–2005.
- [14] D. Park, Y. Hoshi, and C. C. Kemp. “A multi-modal anomaly detector for robot-assisted feeding using an lstm-based variational autoencoder”. In: *IEEE Robotics and Automation Letters* 3.3 (2018), pp. 1544–1551.
- [15] C. Qi and F. Su. “Contrastive-center loss for deep neural networks”. In: *ICIP*. 2017, pp. 2851–2855.
- [16] H. Ren, B. Xu, Y. Wang, et al. “Time-series anomaly detection service at microsoft”. In: *ACM SIGKDD*. 2019, pp. 3009–3017.
- [17] L. Ruff, R. Vandermeulen, N. Goernitz, et al. “Deep one-class classification”. In: *ICML*. 2018, pp. 4393–4402.
- [18] L. Ruff, R. A. Vandermeulen, N. Görnitz, et al. “Deep semi-supervised anomaly detection”. In: *arXiv preprint arXiv:1906.02694* (2019).
- [19] D. T. Shipmon, J. M. Gurevitch, P. M. Piselli, et al. “Time series anomaly detection; detection of anomalous drops with limited features and sparse examples in noisy highly periodic data”. In: *arXiv preprint arXiv:1708.03665* (2017).
- [20] A. Siffer, P.-A. Fouque, A. Termier, et al. “Anomaly detection in streams with extreme value theory”. In: *ACM SIGKDD*. 2017, pp. 1067–1075.
- [21] Y. Su, Y. Zhao, C. Niu, et al. “Robust anomaly detection for multivariate time series through stochastic recurrent neural network”. In: *ACM SIGKDD*. 2019, pp. 2828–2837.
- [22] D. Ulyanov, A. Vedaldi, and V. Lempitsky. “Instance normalization: The missing ingredient for fast stylization”. In: *arXiv preprint arXiv:1607.08022* (2016).
- [23] P. Veličković, G. Cucurull, A. Casanova, et al. “Graph attention networks”. In: *arXiv preprint arXiv:1710.10903* (2017).
- [24] V. Vercruyssen, W. Meert, G. Verbruggen, et al. “Semi-supervised anomaly detection with an application to water analytics”. In: *ICDM*. Vol. 2018. 2018, pp. 527–536.
- [25] T. Wu, F. Chen, and Y. Wan. “Graph attention LSTM network: A new model for traffic flow forecasting”. In: *ICISCE*. 2018, pp. 241–245.
- [26] H. Xiao, D. Guan, R. Zhao, et al. “Semi-supervised Time Series Anomaly Detection Model Based on LSTM Autoencoder”. In: *ICBDS*. 2020, pp. 41–53.
- [27] J. Xie, R. Girshick, and A. Farhadi. “Unsupervised deep embedding for clustering analysis”. In: *ICML*. 2016, pp. 478–487.
- [28] B. Yu, H. Yin, and Z. Zhu. “Spatio-temporal graph convolutional networks: A deep learning framework for traffic forecasting”. In: *arXiv preprint arXiv:1709.04875* (2017).
- [29] H. Zhao, Y. Wang, J. Duan, et al. “Multivariate time-series anomaly detection via graph attention network”. In: *ICDM*. 2020, pp. 841–850.

Supplementary Material

1 Metrics

We reported the precision, recall, and F1 score for label 1. The functions are described as follows:

$$\text{precision}(\text{label} = 1) = \frac{TP(\text{label} = 1)}{TP(\text{label} = 1) + FP(\text{label} = 1)}$$

$$\text{recall}(\text{label} = 1) = \frac{TP(\text{label} = 1)}{TP(\text{label} = 1) + FN(\text{label} = 1)}$$

$$F1 = 2 \times \frac{\text{precision}(\text{label} = 1) \times \text{recall}(\text{label} = 1)}{\text{precision}(\text{label} = 1) + \text{recall}(\text{label} = 1)}$$

where TP is the number of true positives (i.e., the number of correctly predicted label 1), FP is the number of false positives (i.e., the number of incorrectly predicted label 1), and FN is the number of false negatives (i.e., the number of incorrectly predicted label 0).

2 Model Performance

Figure 1 and Figure 2 show the precision and recall comparison between baselines and our method. In general, our method achieved much better performance in precision and recall. We also projected and plotted the embeddings in a 2D space using t-SNE with their labels to demonstrate our approach (see Figure 3).

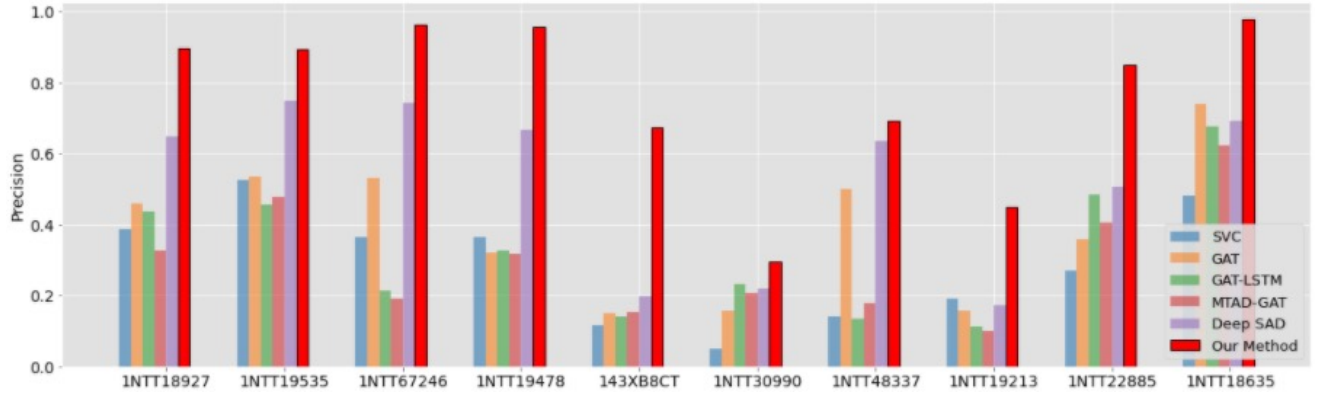


Figure 1: The Precision for baselines and our method (red).

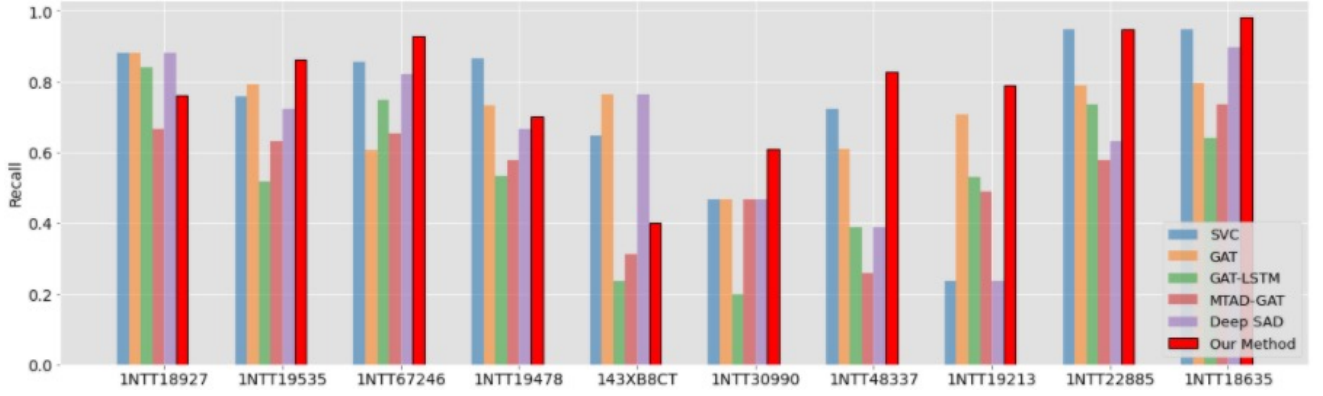


Figure 2: The Recall for baselines and our method (red).

Table 1: Precision and Recall between using different loss functions

Network ID	precision			recall		
	only-CC	only-KL	Ours	only-CC	only-KL	Ours
1NTT18927	0.864	0.735	0.898	0.76	0.7	0.76
1NTT19535	0.913	0.876	0.893	0.724	0.692	0.862
1NTT67246	0.946	0.923	0.963	0.96	0.857	0.929
1NTT19478	0.846	0.897	0.955	0.733	0.693	0.7
143XB8CT	0.667	0.621	0.674	0.353	0.373	0.4
1NTT30990	0.267	0.254	0.294	0.267	0.333	0.611
1NTT48337	0.682	0.629	0.691	0.833	0.722	0.829
1NTT19213	0.333	0.303	0.45	0.576	0.647	0.789
1NTT22885	0.875	0.81	0.85	0.73	0.895	0.949
1NTT18635	0.947	0.95	0.978	0.923	0.974	0.982

Table 2: Precision, Recall, F1 score between using different graph construction methods

Network ID	precision		recall		F1	
	Corr-Graph	Ours	Corr-Graph	Ours	Corr-Graph	Ours
1NTT18927	0.714	0.898	0.746	0.76	0.73	0.823
1NTT19535	0.775	0.893	0.701	0.862	0.736	0.877
1NTT67246	0.85	0.963	0.769	0.929	0.807	0.946
1NTT19478	0.927	0.955	0.577	0.7	0.711	0.808
143XB8CT	0.495	0.674	0.366	0.4	0.421	0.502
1NTT30990	0.184	0.294	0.477	0.611	0.266	0.397
1NTT48337	0.47	0.691	0.614	0.829	0.532	0.754
1NTT19213	0.355	0.45	0.592	0.789	0.444	0.573
1NTT22885	0.553	0.85	0.791	0.949	0.651	0.897
1NTT18635	0.617	0.978	0.86	0.982	0.719	0.980

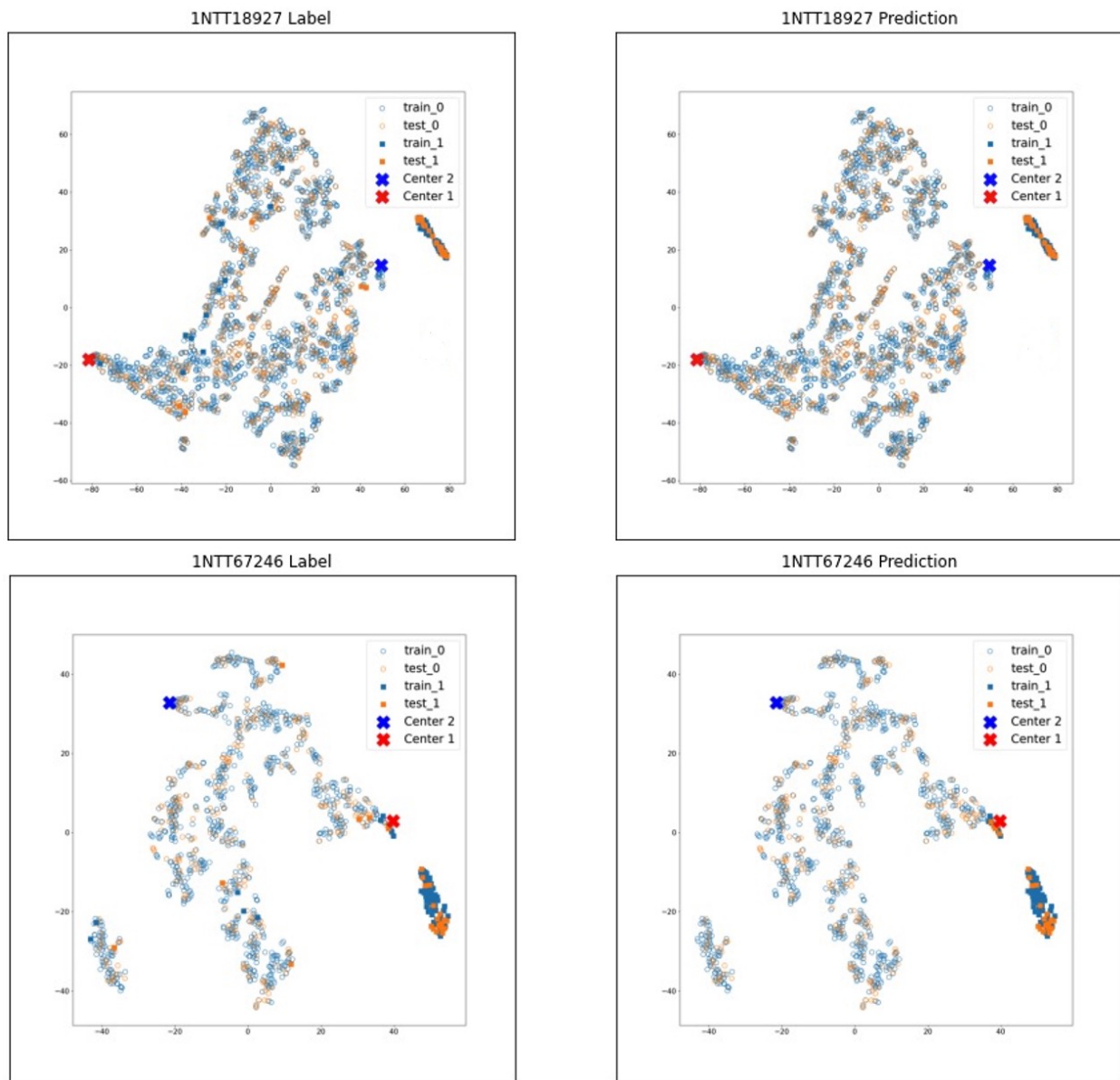


Figure 3: Examples of learned embedding space in 2D for different networks.